One-dimensional simulation of a stirling three-stage pulse-tube refrigerator

EINDHOVEN UNIVERSITY OF TECHNOLOGY
Department of Mathematics and Computer Science

CASA-Report 09-17
May 2009

One-dimensional simulation of a stirling three-stage pulse-tube refrigerator

by

M.A. Etaati, R.M.M. Mattheij,
A.S. Tijsseling, A.T.A.M. de Waele

Centre for Analysis, Scientific computing and Applications
Department of Mathematics and Computer Science
Eindhoven University of Technology
P.O. Box 513
5600 MB Eindhoven, The Netherlands
ISSN: 0926-4507

ONE-DIMENSIONAL SIMULATION OF A STIRLING THREE-STAGE PULSE-TUBE REFRIGERATOR

M.A. Etaati
Department of Mathematics and Computer Science
Eindhoven University of Technology
P.O. Box 513, 5600 MB Eindhoven, The Netherlands
Email: m.a.etaati@tue.nl

R.M.M. Mattheij
Department of Mathematics and Computer Science
Eindhoven University of Technology
P.O. Box 513, 5600 MB Eindhoven, The Netherlands
Email: r.m.m.mattheij@tue.nl

A.S. Tijsseling
Department of Mathematics and Computer Science
Eindhoven University of Technology
P.O. Box 513, 5600 MB Eindhoven, The Netherlands
Email: a.s.tijsseling@tue.nl

A.T.A.M. de Waele
Department of Applied Physics
Eindhoven University of Technology
P.O. Box 513, 5600 MB Eindhoven, The Netherlands
Email: a.t.a.m.d.waele@tue.nl

ABSTRACT

A one-dimensional mathematical model is derived for a three-stage pulse-tube refrigerator (PTR) that is based on the conservation laws and the ideal gas law. The three-stage PTR is regarded as three separate single-stage PTRs that are coupled via proper junction conditions. At the junctions there are six fluid flow possibilities each defining its own boundary conditions for the adjacent domains. Each single stage cools down the gas in the regenerator to a lower temperature such that the system reaches its lowest temperature at the cold end of the third stage. The velocity and pressure amplitudes are decreasing towards the higher stages and there is an essential phase difference between them at different positions. The system of coupled PTRs is solved simultaneously first for the temperatures and then for the velocities and the regenerator pressures. The final result is a robust and accurate simulation tool for the analysis of multi-stage PTR performance.

INTRODUCTION

An innovative technology for cooling down to low temperatures is the so-called pulse-tube refrigerator (PTR). It is applied in medicine and space technology, for example to liquefy nitrogen and to facilitate superconductivity. A typical Stirling single-stage PTR is shown in Fig. 1. The PTR consists of a piston (or compressor) with after-cooler, a regenerator, a cold heat exchanger, a pulse tube, a hot heat exchanger, an orifice and a reservoir, in this sequence. The piston maintains an oscillating helium flow in the regenerator-tube system. The temperature of the helium increases when the flow is compressed and moving towards the hot heat exchanger (HHX) into the reservoir. The gas cools down when the flow is decompressed and moving back towards the cold heat exchanger (CHX) into the regenerator. The heat absorbing features of the regenerator, which is a porous medium with large heat capacity and large heat-exchanging surface, results in net cooling power per cycle. The cooling takes place at the cold heat exchanger, which is placed in a vacuum chamber. See [1, 2] for more explanation and analysis.

For reaching temperatures below 30 K a multi-stage PTR can be useful. Several single PTR are placed in series, such that the cold end of one stage is cooling the helium that enters the regenerator of the next stage. Each single PTR has dimensions and materials fitted for its intended temperature range. The studied three-stage pulse-tube refrigerator is sketched in Fig. 2. Its dimensions and properties are listed in the Appendix.

In this paper we derive a mathematical model that will be the basis for numerical simulation of the PTR. All parts of the system are coupled together in a physically correct way. The study is based on previous work [3, 4], but now extended to modelling the regenerator and multi-staging.

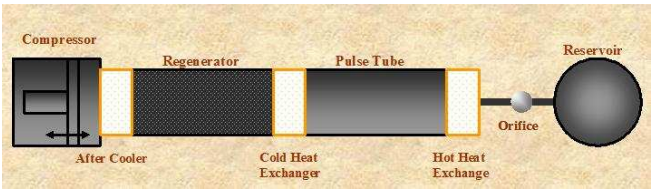

Figure 1. SINGLE-STAGE STIRLING PULSE-TUBE REFRIGERATOR.

MATHEMATICAL MODEL

To analyse the fluid flow and heat transfer inside a single-stage PTR, we consider the fluid as a continuum. The heat exchangers are assumed ideal. The basic equations are the three laws of conservation and the equation of state of an ideal gas. The material properties are taken constant herein.

The Tube Model

Consider a one-dimensional region $0 < x < L_t$, where L_t is the length of the tube. The four basis equations for the tube have the following dimensional form [4]

$$\frac{\partial \rho_g}{\partial t} + \frac{\partial}{\partial x}(\rho_g u) = 0, \tag{1}$$

$$\rho_g(\frac{\partial u}{\partial t} + u\frac{\partial u}{\partial x}) = -\frac{\partial p}{\partial x} + \frac{4}{3}\mu\frac{\partial^2 u}{\partial x^2}, \tag{2}$$

$$\rho c_g(\frac{\partial T_g}{\partial t} + u\frac{\partial T_g}{\partial x}) = \frac{\partial p}{\partial t} + u\frac{\partial p}{\partial x} + k_g\frac{\partial^2 T_g}{\partial x^2} + \frac{4}{3}\mu(\frac{\partial u}{\partial x})^2, \tag{3}$$

$$p = \rho_g R_m T_g. \tag{4}$$

The symbols are defined in the Appendix. The equations are made non-dimensional by proper scaling parameters [5]. Employing asymptotic analysis, we see that the pressure p_t in the tube is uniform and we set it equal to the pressure at the interface with the regenerator. By eliminating the density, the following simplified continuity equation for the dimensionless velocity u_t and energy equation for the dimensionless temperature T_{g_t} are obtained

$$\frac{\partial u_t}{\partial x} = (\frac{a_1}{p_t})\frac{\partial^2 T_{g_t}}{\partial x^2} - (\frac{1}{\gamma p_t})\frac{\partial p_t}{\partial t}, \tag{5}$$

$$\frac{\partial T_{g_t}}{\partial t} = a_2(\frac{T_{g_t}}{p_t})\frac{\partial^2 T_{g_t}}{\partial x^2} - u_t\frac{\partial T_{g_t}}{\partial x} + (1-\gamma)\frac{\partial u_t}{\partial x}T_{g_t}, \tag{6}$$

where $a_1 = 1/BPe_g$ and $a_2 = \gamma/BPe_g$. The temperature equation (6) is a nonlinear convection-diffusion equation. The coefficient of the diffusion term is very small, $a_2 \ll 1$, so that the flow is highly dominated by convection. The dimensional volume flow

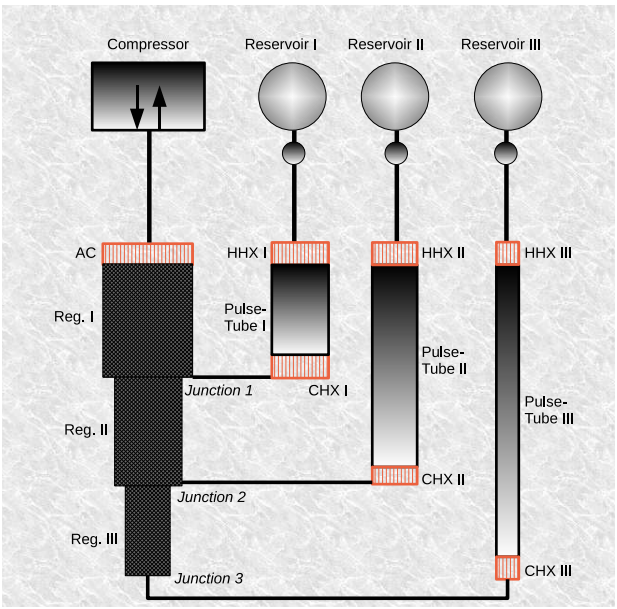

Figure 2. THREE-STAGE STIRLING PULSE-TUBE REFRIGERATOR.

$\dot{V}_{\rm H}$ or the velocity $u_{\rm H}$ through the orifice is in a linear approximation given by [2]

$$\dot{V}_{\rm H}(t) = C_{\rm or}(p_- p_{\rm b}), \tag{7}$$

where $p_{\rm b}$ is the buffer (reservoir) pressure and $C_{\rm or}$ is the flow conductance of the orifice. The following non-dimensional relation gives the velocity at the hot end of the tube as the boundary condition (BC) for the velocity equation (5)

$$u_{\rm H}(t) = \mathcal{C}(p - \mathcal{E}_0), \tag{8}$$

where $\mathcal{E}_0 = p_b/p_{av}$. The upwind BC for the temperature equation (6) depend on the local flow directions and read

$$\begin{cases} T_{g_t}(L_t,t) = T_{\rm H} \quad \text{if} \quad u_t(L_t,t) \le 0, \\ \dfrac{\partial T_{g_t}}{\partial x}(L_t,t) = [(1-\gamma)\dfrac{\partial u_t}{\partial x}T_{g_t}(L_t,0) - \dfrac{\partial T_{g_t}}{\partial t}(L_t,t)]/u_t(L_t,t) \\ \qquad\qquad\qquad\qquad \text{if} \quad u_t(L_t,t) > 0. \end{cases} \tag{9}$$

$$\begin{cases} T_{g_t}(0,t) = T_{\rm C} \quad \text{if} \quad u_t(0,t) \ge 0, \\ \dfrac{\partial T_{g_t}}{\partial x}(0,t) = [(1-\gamma)\dfrac{\partial u_t}{\partial x}T_{g_t}(0,t) - \dfrac{\partial T_{g_t}}{\partial t}(0,t)]/u_t(0,t) \\ \qquad\qquad\qquad\qquad \text{if} \quad u_t(0,t) < 0. \end{cases} \tag{10}$$

where T_H and T_C are the given temperatures at the hot and cold ends respectively.

The Regenerator Model

The governing equations for the regenerator, where $0 < x < L_r$, are similar to those of the tube and read [5]

$$\frac{\partial \rho_g}{\partial t} + \frac{\partial}{\partial x}(\rho_g u) = 0, \tag{11}$$

$$\rho_g(\frac{\partial u}{\partial t} + u\frac{\partial u}{\partial x}) = -\frac{\partial p}{\partial x} + \frac{4}{3}\mu\frac{\partial^2 u}{\partial x^2} - \frac{\mu}{\phi k}u, \tag{12}$$

$$\rho_r(1-\phi)c_r\frac{\partial T_r}{\partial t} = \beta(T_g - T_r) + (1-\phi)k_r\frac{\partial^2 T_r}{\partial x^2}, \tag{13}$$

$$\rho_g c_g \phi\frac{dT_g}{dt} = \beta(T_r - T_g) + \phi(\frac{\partial p}{\partial t} + u\frac{\partial p}{\partial x}) + \phi k_g\frac{\partial^2 T_g}{\partial x^2} + \frac{4}{3}\mu(\frac{\partial u}{\partial x})^2, \tag{14}$$

$$p = \rho_g R_m T_g, \tag{15}$$

where ϕ is the porosity of the regenerator material which is assumed to be constant. The flow resistance is taken into account by Darcy's law via the momentum equation (12). By non-dimensionalising the variables and employing asymptotic analysis, the equations take the following simplified form:

$$\frac{\partial u_r}{\partial x} = \frac{a_1}{p_r}\frac{\partial^2 T_{g_r}}{\partial x^2} + \frac{a_6}{p_r}(T_r - T_{g_r}) + a_7(\frac{u_r}{p_r})u_r - \frac{1}{\gamma p_r}\frac{\partial p_r}{\partial t}, \tag{16}$$

$$\frac{\partial p_r}{\partial x} = -\mathcal{D}u_r, \tag{17}$$

$$\frac{\partial T_r}{\partial t} = a_3(T_{g_r} - T_r) + a_4\frac{\partial^2 T_r}{\partial x^2}, \tag{18}$$

$$\frac{\partial T_{g_r}}{\partial t} = a_2(\frac{T_{g_r}}{p_r})\frac{\partial^2 T_{g_r}}{\partial x^2} + a_5(\frac{T_{g_r}}{p_r})(T_r - T_{g_r}) + (1-\gamma)\frac{\partial u_r}{\partial x}T_{g_r} - u_r\frac{\partial T_{g_r}}{\partial x}, \tag{19}$$

where $a_3 = \mathcal{F}/c_r$, $a_4 = 1/c_r Pe_r$, $a_5 = \mathcal{E}\gamma/B$, $a_6 = \mathcal{E}/B$ and $a_7 = \mathcal{D}/\gamma$. Note that T_r is the temperature of the regenerator material and T_{g_r} is the gas temperature inside the regenerator. All other parameters are given in the Appendix. The pressure p_c at the compressor side gives a BC for Eq. (17), namely $p_c = p_{av} - \overline{p}\sin(\omega t)$. For the gas temperature equation (19), which is a convection-diffusion equation, we introduce two velocity-dependent boundary conditions similar to the equations (9-10) as follows

$$\begin{cases} T_{g_r}(0,t) = T_H \quad \text{if} \quad u_r(0,t) \geq 0, \\ \dfrac{\partial T_{g_r}}{\partial x} = [a_5(\dfrac{T_{g_r}}{p_r})(T_r - T_{g_r}) + (1-\gamma)\dfrac{\partial u_r}{\partial x}T_{g_r} - \dfrac{\partial T_{g_r}}{\partial t}]/u_r(0,t) \\ \qquad\qquad\qquad\qquad \text{if} \quad u_r(0,t) < 0, \end{cases} \tag{20}$$

$$\begin{cases} T_{g_r}(L_r,t) = T_C \quad \text{if} \quad u_r(L_r,t) \leq 0, \\ \dfrac{\partial T_{g_r}}{\partial x} = [a_5(\dfrac{T_{g_r}}{p_r})(T_r - T_{g_r}) + (1-\gamma)\dfrac{\partial u_r}{\partial x}T_{g_r} - \dfrac{\partial T_{g_r}}{\partial t}]/u_r(L_r,t) \\ \qquad\qquad\qquad\qquad \text{if} \quad u_r(L_r,t) > 0. \end{cases} \tag{21}$$

We apply the heat exchanger temperatures as the proper BC for the material temperature equation (18). Mass conservation at the cold end gives BC for the velocity equation (16).

The Three-Stage PTR Model

The three-stage PTR (Fig. 2) is treated as three single-stage PTRs that are coupled via physical interface conditions. The regenerator material temperatures are considered to be fully decoupled from each other. The local energy and mass conservation provide the coupling conditions for the gas velocities and gas temperatures at the interfaces. For instance, at the junction connecting the first regenerator, the second regenerator and the first pulse-tube, we have mass conservation according to

$$\dot{m}_{Reg1} = \dot{m}_{Reg2} + \dot{m}_{Tube1}, \tag{22}$$

which is equivalent with

$$\frac{uA\phi}{T}|_{Reg1} = \frac{uA\phi}{T}|_{Reg2} + \frac{uA}{T}|_{Tube1}. \tag{23}$$

Neglecting the kinetic energy and local conduction terms, the energy conservation is satisfied by the enthalpy flow condition

$$H^*|_{Reg1} = H^*|_{Reg2} + H^*|_{Tube1}, \tag{24}$$

with

$$H^* = n^* H_m, \tag{25}$$

where n^* is the molar flow and H_m is the molar enthalpy. Then

$$n^* = \frac{uA}{V_m} = \frac{uAp}{RT}, \tag{26}$$

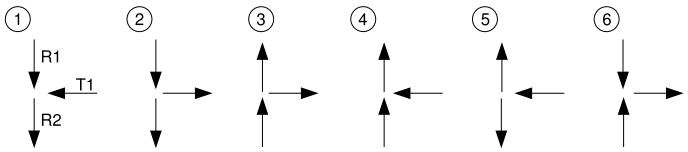

Figure 3. SIX FLUID FLOW POSSIBILITIES AT JUNCTION.

where V_m is the molar volume, R is the gas constant and p is the thermodynamic pressure. The molar enthalpy is

$$H_m^* = c_p T. \tag{27}$$

The enthalpy flow is then

$$H^* = (\frac{c_p p}{R}) uA. \tag{28}$$

Therefore energy conservation at the junction reduces to volume conservation

$$uA\phi|_{Reg1} = uA\phi|_{Reg2} + uA|_{Tube1}. \tag{29}$$

By using mass conservation (Eq. 23) and energy conservation (Eq. 29) together with pressure continuity we couple two regenerators and one pulse-tube at each junction. Equation (23) is simply used as the proper BC for the upper regenerator at each junction.
There are six (out of eight) flow possibilities at an incompressible junction as depicted in Fig. 3. The vertical arrows show the flow in two consecutive regenerators and the horizontal one displays the flow to or from the pulse-tube. These multiple flows are explained below and the corresponding upwind boundary conditions for the temperature equations (6) and (19) are listed in Table 1.

State I: There are two outflows: from the upper regenerator and from the tube. These are described by the Neumann BCs (Eq. 10) and (Eq. 21) respectively. Temperature-dependant mass inflow Eq.(23) is used as the BC for the lower regenerator.

State II: We apply Neumann BC (Eq. 21) for the upper regenerator. Mass inflow Eq.(23) is the BC for the lower regenerator. The gas in the tube takes the temperature of the upper regenerator.

Table 1. BOUNDARY CONDITIONS AT THE JUNCTION ACCORDING TO DIFFERENT STATES. D:=Dirichlet; N:=Neumann

state	Regenerator I	Regenerator II	Pulse-Tube I
1	N. (outflow)	D. (inflow)	N. (outflow)
2	N. (outflow)	D. (inflow)	D. (inflow)
3	D. (inflow)	N. (inflow)	D. (inflow)
4	D. (inflow)	N. (outflow)	N. (outflow)
5	D. (inflow)	D. (inflow)	N. (outflow)
6	N. (outflow)	N. (outflow)	D. (inflow)

State III: We apply Neumann BC (Eq. 10) for the lower regenerator and mass inflow for the upper regenerator. The gas temperature of the tube at the junction is equal to the one in the lower regenerator.

State IV: There are two outflows, from lower regenerator and tube, and we apply the Neumann BCs (Eq. 10) and (Eq. 21) to them. Mass conservation (Eq. 23) is applied to the junction and this gives the BC for the upper regenerator.

State V: In this state, which lasts a very short time during the gas circulation, Neumann BC (Eq. 10) is applied to the pulse-tube and the gas temperature of the regenerators is taken equal to the gas temperature of the pulse-tube at the junction.

State VI: In this flow situation, which also lasts for a very short time, the flow from both regenerators enters the pulse-tube. Mass inflow according to (Eq.23) is then defined to the junction as the BC for the pulse-tube. Two Neumann BCs for the gas temperatures are applied to the outflows from the regenerators.

The simulation starts from linear functions for the initial temperatures in the regenerators. Third degree polynomials are used for the initial temperatures of the tubes. These are derived from estimates of the flow amplitudes at the cold and hot ends of the tubes. The initial temperatures at the cold heat exchangers, CHX I and CHX II are estimated. The temperature of CHX III is set as a constant value.

NUMERICAL METHOD

The energy equations for the gas temperature in the tubes (6), the gas and the material temperatures in the regenerators (18-19) are solved simultaneously for all three stages by an implicit method of lines. The equations are discretised in space using one-sided differences of second-order accuracy and flux limiters for the convection terms. The θ-method with $\theta = 0.5 + \Delta t$ gives

second-order accuracy in time. For instance, the discretisation of Eq. (6) for $u_j^n > 0$ and omitting the subscript t is

$$
\begin{aligned}
&T_{\mathrm{g}_j}^{n+1} - \triangle t^n \theta \\
&\left(\varepsilon_2(\frac{T_{\mathrm{g}_j}^n}{p_j^n}) \frac{T_{\mathrm{g}_{j-1}}^{n+1} - 2T_{\mathrm{g}_j}^{n+1} + T_{\mathrm{g}_{j+1}}^{n+1}}{h^2} + (1-\gamma) T_{\mathrm{g}_j}^n \frac{u_{j+1}^{n+1} - u_{j-1}^{n+1}}{2h} \right) = \\
&T_{\mathrm{g}_j}^n + (1-\theta)\triangle t^n \\
&\left(\varepsilon_2(\frac{T_{\mathrm{g}_j}^n}{p_j^n}) \frac{T_{\mathrm{g}_{j-1}}^n - 2T_{\mathrm{g}_j}^n + T_{\mathrm{g}_{j+1}}^n}{h^2} + (1-\gamma) T_{\mathrm{g}_j}^n \frac{u_{j+1}^n - u_{j-1}^n}{2h} \right) \\
&-c_j^n \left(1 + \frac{1}{2}(1-c_j^n) \left(\frac{\Phi_{j+\frac{1}{2}}^n}{r_{j+\frac{1}{2}}^n} - \Phi_{j-\frac{1}{2}}^n \right) \right) (T_{\mathrm{g}_j}^n - T_{\mathrm{g}_{j-1}}^n),
\end{aligned}
\tag{30}
$$

where the Courant number $c_j^n := \triangle t^n u_j^n / \triangle x$ and $\triangle t^n$ is an adaptive time step satisfying condition (32). The ratio $r_{j+\frac{1}{2}}^n$ is defined by

$$
r_{j+\frac{1}{2}}^n := \begin{cases} \dfrac{T_{g_j}^n - T_{g_{j-1}}^n}{T_{g_{j+1}}^n - T_{g_j}^n} & \text{if } u_j^n > 0, \\ \dfrac{T_{g_{j+2}}^n - T_{g_{j+1}}^n}{T_{g_{j+1}}^n - T_{g_j}^n} & \text{if } u_j^n < 0. \end{cases} \tag{31}
$$

The flux limiter $\Phi_{j+\frac{1}{2}}^n = \Phi(r_{j+\frac{1}{2}}^n)$ herein is that of Van Leer, see [6]. For $r \leq 0$ the limiter function $\Phi(r) = 0$. Because of the CFL stability condition $|c_j^n| \leq 1$ it is required that

$$
\triangle t^n \leq \triangle x / \max_j |u_j^n|. \tag{32}
$$

The continuity equation (5) is discretised with second order of accuracy as follows

$$
\begin{aligned}
&u_{N_x}^{n+1} = u_{\mathrm{H}}^{n+1}, && j = N_x, \\
&u_{j+1}^{n+1} - u_{j-1}^{n+1} = \frac{2\varepsilon_1}{h}(T_{\mathrm{g}_{j-1}}^{n+1} - 2T_{\mathrm{g}_j}^{n+1} + T_{\mathrm{g}_{j+1}}^{n+1}) \\
&-\frac{h}{\gamma p_j^n}(\frac{3p_j^{n+1} - 4p_j^n + p_j^{n-1}}{\Delta t}), && j = 2, \ldots, N_x - 1, \\
&-3u_1^{n+1} + 4u_2^{n+1} - u_3^{n+1} = \frac{2\varepsilon_1}{h}(T_{\mathrm{g}_3}^{n+1} - 2T_{\mathrm{g}_2}^{n+1} + T_{\mathrm{g}_1}^{n+1}) \\
&-\frac{h}{\gamma p_1^n}(\frac{3p_1^{n+1} - 4p_1^n + p_1^{n-1}}{\Delta t}), && j = 1,
\end{aligned}
\tag{33}
$$

for every time level $n = 0, 1, 2, 3, \ldots$ with u_{H} given by Eq. (8). The pulse-tubes and regenerators are coupled by the interface conditions Eq.(23) and Eq.(29). The global system of equations for the temperatures that is numerically solved reads

$$
\begin{bmatrix}
\mathbf{X} & \mathbf{X} & \mathbf{C} & \mathbf{C} & \mathbf{0} & \mathbf{0} & \mathbf{0} & \mathbf{0} & \mathbf{0} & \mathbf{0} \\
\mathbf{X} & \mathbf{X} & \mathbf{0} & \mathbf{0} & \mathbf{0} & \mathbf{0} & \mathbf{0} & \mathbf{0} & \mathbf{0} & \mathbf{0} \\
\mathbf{C} & \mathbf{0} & \mathbf{X} & \mathbf{0} & \mathbf{0} & \mathbf{0} & \mathbf{0} & \mathbf{0} & \mathbf{0} & \mathbf{0} \\
\mathbf{C} & \mathbf{0} & \mathbf{0} & \mathbf{X} & \mathbf{X} & \mathbf{C} & \mathbf{C} & \mathbf{0} & \mathbf{0} & \mathbf{0} \\
\mathbf{0} & \mathbf{X} & \mathbf{0} & \mathbf{X} & \mathbf{X} & \mathbf{0} & \mathbf{0} & \mathbf{C} & \mathbf{0} & \mathbf{0} \\
\mathbf{0} & \mathbf{0} & \mathbf{0} & \mathbf{C} & \mathbf{0} & \mathbf{X} & \mathbf{0} & \mathbf{0} & \mathbf{0} & \mathbf{0} \\
\mathbf{0} & \mathbf{0} & \mathbf{0} & \mathbf{C} & \mathbf{0} & \mathbf{0} & \mathbf{X} & \mathbf{X} & \mathbf{0} & \mathbf{0} \\
\mathbf{0} & \mathbf{0} & \mathbf{0} & \mathbf{0} & \mathbf{C} & \mathbf{0} & \mathbf{X} & \mathbf{X} & \mathbf{0} & \mathbf{0} \\
\mathbf{0} & \mathbf{0} & \mathbf{0} & \mathbf{0} & \mathbf{0} & \mathbf{0} & \mathbf{0} & \mathbf{0} & \mathbf{C} & \mathbf{X}
\end{bmatrix}
\begin{bmatrix}
\mathbf{T}_{g_{R1}} \\ \mathbf{T}_{R1} \\ \mathbf{T}_{g_{Tube1}} \\ \mathbf{T}_{g_{R2}} \\ \mathbf{T}_{R2} \\ \mathbf{T}_{g_{Tube2}} \\ \mathbf{T}_{g_{R3}} \\ \mathbf{T}_{R3} \\ \mathbf{T}_{g_{Tube3}}
\end{bmatrix}^{n+1}
=
\begin{bmatrix}
\mathcal{F}_1 \\ \mathcal{F}_2 \\ \mathcal{F}_3 \\ \mathcal{F}_4 \\ \mathcal{F}_5 \\ \mathcal{F}_6 \\ \mathcal{F}_7 \\ \mathcal{F}_8 \\ \mathcal{F}_9
\end{bmatrix}^{n}
\tag{34}
$$

where **X** represents the discretisation of a single PTR, and **C** accounts for the coupling at the junctions. The global system of equations for the velocities and the regenerator pressures that is numerically solved reads

$$
\begin{bmatrix}
\mathbf{X} & \mathbf{X} & \mathbf{C} & \mathbf{C} & \mathbf{0} & \mathbf{0} & \mathbf{0} & \mathbf{0} & \mathbf{0} & \mathbf{0} \\
\mathbf{X} & \mathbf{X} & \mathbf{0} & \mathbf{0} & \mathbf{0} & \mathbf{0} & \mathbf{0} & \mathbf{0} & \mathbf{0} & \mathbf{0} \\
\mathbf{0} & \mathbf{C} & \mathbf{X} & \mathbf{0} & \mathbf{0} & \mathbf{0} & \mathbf{0} & \mathbf{0} & \mathbf{0} & \mathbf{0} \\
\mathbf{0} & \mathbf{0} & \mathbf{0} & \mathbf{X} & \mathbf{X} & \mathbf{C} & \mathbf{C} & \mathbf{0} & \mathbf{0} & \mathbf{0} \\
\mathbf{0} & \mathbf{C} & \mathbf{0} & \mathbf{X} & \mathbf{X} & \mathbf{0} & \mathbf{0} & \mathbf{0} & \mathbf{0} & \mathbf{0} \\
\mathbf{0} & \mathbf{0} & \mathbf{0} & \mathbf{0} & \mathbf{C} & \mathbf{X} & \mathbf{0} & \mathbf{0} & \mathbf{0} & \mathbf{0} \\
\mathbf{0} & \mathbf{0} & \mathbf{0} & \mathbf{C} & \mathbf{0} & \mathbf{0} & \mathbf{X} & \mathbf{X} & \mathbf{C} & \mathbf{0} \\
\mathbf{0} & \mathbf{0} & \mathbf{0} & \mathbf{0} & \mathbf{C} & \mathbf{0} & \mathbf{X} & \mathbf{X} & \mathbf{0} & \mathbf{0} \\
\mathbf{0} & \mathbf{0} & \mathbf{0} & \mathbf{0} & \mathbf{0} & \mathbf{0} & \mathbf{0} & \mathbf{C} & \mathbf{X} & \mathbf{0}
\end{bmatrix}
\begin{bmatrix}
\mathbf{u}_{R1} \\ \mathbf{p}_{R1} \\ \mathbf{u}_{Tube1} \\ \mathbf{u}_{R2} \\ \mathbf{p}_{R2} \\ \mathbf{u}_{Tube2} \\ \mathbf{u}_{R3} \\ \mathbf{p}_{R3} \\ \mathbf{u}_{Tube3}
\end{bmatrix}^{n+1}
=
\begin{bmatrix}
\mathcal{F}_1 \\ \mathcal{F}_2 \\ \mathcal{F}_3 \\ \mathcal{F}_4 \\ \mathcal{F}_5 \\ \mathcal{F}_6 \\ \mathcal{F}_7 \\ \mathcal{F}_8 \\ \mathcal{F}_9
\end{bmatrix}^{n}
. \tag{35}
$$

RESULTS and DISCUSSION

A three-stage PTR operating at 20 Hz has been simulated for a set lowest temperature of 4 K. All parameters are listed in the Appendix. In Fig. 4 we see the velocities at different positions for all three stages. Fig. 5 shows the pressure at different positions in the pulse-tube refrigerator. The amplitude of velocity and pressure decreases with distance from the compressor, and there is a phase difference between all signals. The pressure drop is caused by the resistance of the regenerators and the velocity decrease is caused by the compressibility and the decrease of temperature and pressure per tube. Fig. 6 and 7 give the temperatures at the cold and hot ends of the tubes. At the hot end, in the decompression phase, gas flows from the buffer via the orifice and carries the room temperature T_{H} as it enters the pulse-tube. In the compression phase, as soon as the uniform pressure in the tube becomes higher than the pressure in the buffer, the gas is approaching the HHX with a temperature higher than the boundary temperature T_{H} (BC (9)). At the cold end the gas enters the tube via the CHX with temperature T_{C} and at a pressure higher than

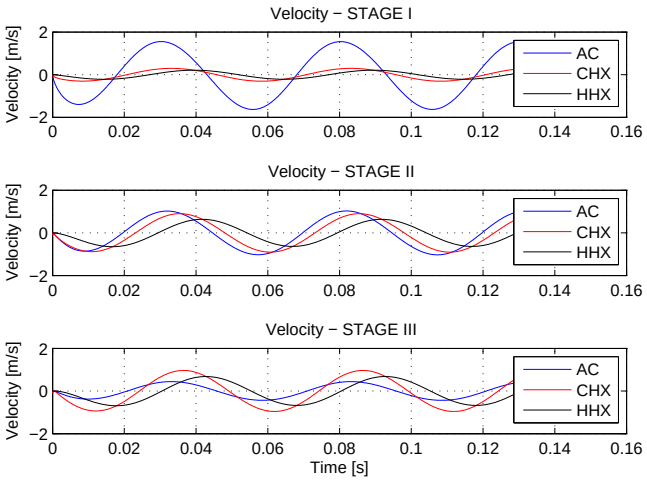

Figure 4. Velocity variation in the three-stage PTR.

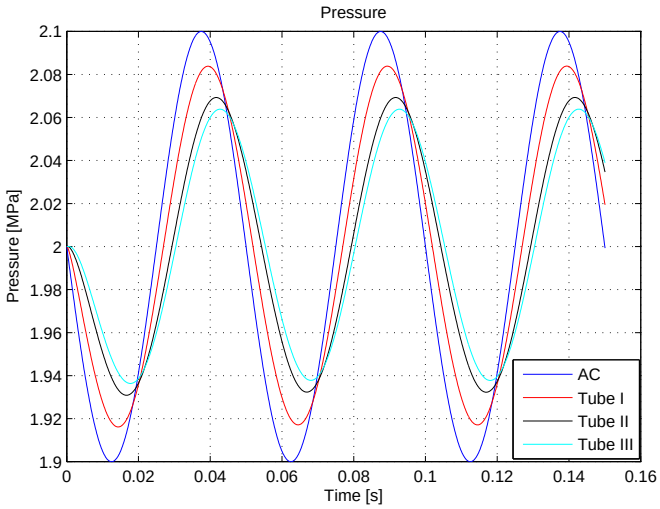

Figure 5. Pressure variation in the three-stage PTR.

the buffer pressure and returns to the CHX at a lower pressure with a temperature lower than T_C (BC (10)). This below-T_C temperature generates the desired cooling power. When the pressure and the velocity at the cold end of the third stage are in phase the maximum cooling power occurs. The cooling power is equal to the cycle-averaged enthalpy flow [1, 2]

$$\overline{\dot{H}} = \frac{1}{t_c}\int_t^{t+t_c} c_p \dot{m}_t T_g dt, \tag{36}$$

with

$$\dot{m}_t = A_t \rho_g u_t,$$

where t_c is the cycle period. In Refs [1, 2] this quantity is estimated by

$$\overline{\dot{H}}_e = \frac{1}{2} C_{or} \bar{p}^2, \tag{37}$$

where $\bar{p}$ is the pressure amplitude which differs per tube. The calculated values are 4.37 W, 0.67 W and 0.46 W for the first, the second and the third tube, respectively. The corresponding estimated values 4.26 W, 0.86 W and 0.43 W are consistent. The calculated enthalpy flows in the three tubes are shown in Fig. 8.

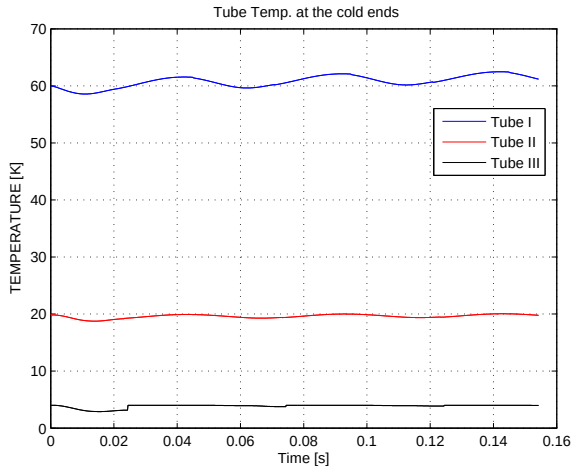

Figure 6. Cold end temperatures in the three-stage PTR.

CONCLUSION

A mathematical model has been developed that describes the heat and mass transfer in a three-stage pulse-tube refrigerator where the hot and cold heat exchangers are assumed to be ideal. The system is operating at frequencies higher than usual. In the coupling of single-stage PTRs, six fluid flow possibilities at the junctions have been considered. Each flow possibility led to its own set of upwind BCs. The studied three-stage PTR is able to cool down to 4 K with a remaining cooling power of about 0.5 W. Real gas in the third stage, temperature-dependant material properties and double inlets are essential features that have not been considered herein.

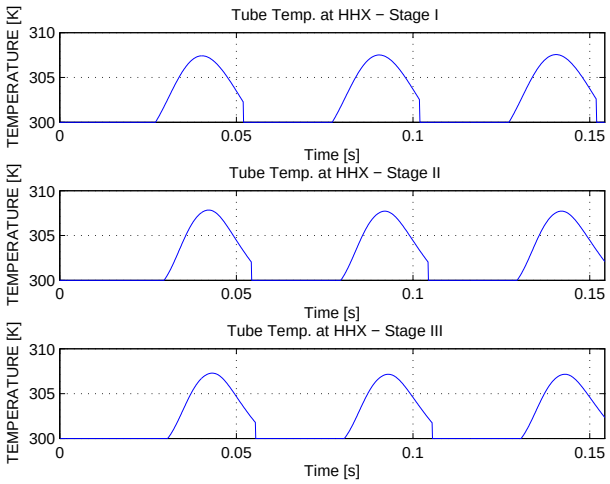

Figure 7. Hot end temperatures in the three-stage PTR.

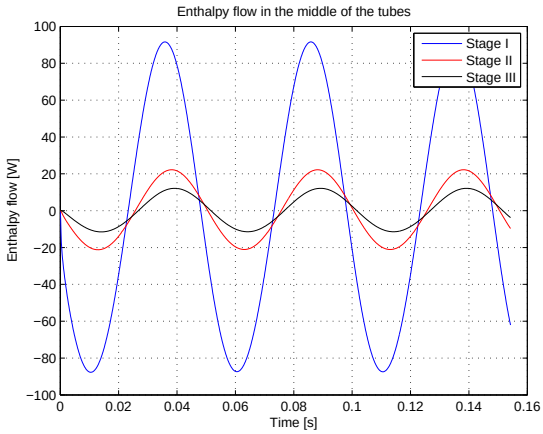

Figure 8. Enthalpy flow in middle of three pulse-tubes.

ACKNOWLEDGMENT

This project is funded by STW (Dutch Technology Foundation). The grant number is ETF6595.

REFERENCES

[1] de Waele A T A M, Steijaert P P, Gijzen J. *Thermodynamical aspects of pulse tubes*, Cryogenics 1997(37):313-324.

[2] de Waele A T A M, Steijaert P P, Koning J J. *Thermodynamical aspects of pulse tubes II*, Cryogenics 1998(38):329-335.

[3] Lyulina I A, Mattheij R M M, Tijsseling A S, de Waele A T A M. *Numerical simulation of pulse-tube refrigerators*, International Journal of Nonlinear Sciences and Numerical Simulations, 2004(5):79-88, Corrigenda: 2004(5):287.

[4] Lyulina I A. *Numerical simulation of pulse-tube refrigerators*. PhD Thesis, Eindhoven University of Technology, Dept. of Math. and Computer Science, 2005. Available from http://alexandria.tue.nl/extra2/200510289.pdf.

[5] Smith W R. *One-dimensional models for heat and mass transfer in pulse tube refrigerators*, Cryogenics 2001(41):573-582.

[6] Mattheij R M M, Rienstra S W, ten Thije Boonkkamp J H M. *Partial Differential Equations, Modeling, Analysis, Computing*, SIAM Press: Philadelphia, 2005:396.

Appendix: PHYSICAL DATA FOR THE THREE-STAGE PULSE-TUBE REFRIGERATOR.

Table 2. GEOMETRIES.

Symbol	Definition	Value
d_{t1}	diameter of the 1^{st} tube	24.6 mm
d_{t2}	diameter of the 2^{nd} tube	7 mm
d_{t3}	diameter of the 3^{rd} tube	5 mm
d_{r1}	diameter of the 1^{st} regenerator	72 mm
d_{r2}	diameter of the 2^{nd} regenerator	32 mm
d_{r3}	diameter of the 3^{rd} regenerator	19 mm
L_{t1}	length of the 1^{st} tube	67.5 mm
L_{t2}	length of the 2^{nd} tube	246 mm
L_{t3}	length of the 3^{rd} tube	285 mm
L_{r1}	length of the 1^{st} regenerator	65 mm
L_{r2}	length of the 2^{nd} regenerator	78.5 mm
L_{r3}	length of the 3^{rd} regenerator	70 mm

Table 3. REGENERATOR MATERIAL PROPERTIES.

Symbol	Definition	Value
Material kind	1^{st} regenerator	Stainless Steel
Material kind	2^{nd} regenerator	Lead
Material kind	3^{rd} regenerator	ErNi
$\overline{c}_r$	reg. specific heat capacity	400 J kg^{-1} K^{-1}
k	reg. permeability	3.0×10^{-11} m^2
$\overline{k}_g$	gas thermal conductivity	1.58×10^{-1} W m^{-1} K^{-1}
$\overline{k}_{r1}$	1^{st} reg. thermal conductivity	10 W m^{-1} K^{-1}
$\overline{k}_{r2}$	2^{nd} reg. thermal conductivity	5 W m^{-1} K^{-1}
$\overline{k}_{r3}$	3^{rd} reg. thermal conductivity	5 W m^{-1} K^{-1}
ρ_{r1}	1^{st} reg. density	7800 kg m^{-3}
ρ_{r2}	2^{nd} reg. density	11350 kg m^{-3}
ρ_{r3}	3^{rd} reg. density	9400 kg m^{-3}
ϕ_1	1^{st} reg. porosity	0.682
ϕ_2	2^{nd} reg. porosity	0.6
ϕ_3	3^{rd} reg. porosity	0.6
β	reg. heat transfer coefficient	10^8 W m^{-3} K^{-1}

Table 4. GENERAL PROPERTIES.

Symbol	Definition	Value
f	frequency	20 s^{-1}
α	orifice setting parameter [2]	1
C_{or1}	$L_{t1}\omega/\gamma\alpha\overline{u}$	1.21^{-9} m^3 Pa^{-1}s^{-1}
C_{or2}	$L_{t2}\omega/\gamma\alpha\overline{u}$	3.57^{-10} m^3 Pa^{-1}s^{-1}
C_{or3}	$L_{t3}\omega/\gamma\alpha\overline{u}$	2.11^{-10} m^3 Pa^{-1}s^{-1}
c_p	gas specific heat capacity	5.2×10^3 J kg^{-1}K^{-1}
$\overline{p}$	pressure oscillation amplitude	10^5 Pa
p_{av}	average pressure	2×10^6 Pa
R	gas constant	8.4 J mol^{-1}K^{-1}
R_m	specific gas constant	2.1×10^3 J kg^{-1}K^{-1}
T_a	ambient temperature	300 K
T_H	hot temperature	300 K
$\overline{u}$	gas velocity	1.0 m s^{-1}
V_{b1}	1^{st} buffer volume	1×10^{-3} m^3
V_{b2}	2^{nd} buffer volume	1×10^{-3} m^3
V_{b3}	3^{rd} buffer volume	1×10^{-3} m^3
ω	angular frequency	125.66 s^{-1}
$\overline{\rho}$	gas density	4.7 kg m^{-3}
$\overline{\mu}$	gas dynamic viscosity	10^{-5} Pa s

Table 5. DIMENSIONLESS NUMBERS AND VALUES.

Symbol	Definition	Value
$\mathcal{B}$	$p_{av}/\overline{\rho}R_mT_a$	0.675
$\mathcal{C}_1$	$C_{or1}p_{av}/A_{t1}\overline{u}$	5.089
$\mathcal{C}_2$	$C_{or2}p_{av}/A_{t2}\overline{u}$	18.553
$\mathcal{C}_3$	$C_{or3}p_{av}/A_{t3}\overline{u}$	21.49
$\mathcal{D}$	$k\overline{\mu}\overline{u}^2/\phi p_{av}\omega k$	2.2×10^{-3}
$\mathcal{E}$	$\beta/\overline{\rho}c_g\phi\omega$	47.74
$\mathcal{E}_0$	$\overline{p}_b/p_{av}$	1.0008
$\mathcal{F}$	$\beta/[\rho_r\overline{c}_r(1-\phi)\omega]$	1.604
Pe_{r1}	$\rho_{r1}\overline{c}_r\overline{u}^2/\overline{k}_{r1}\omega$	1.24×10^3
Pe_{r2}	$\rho_{r2}\overline{c}_r\overline{u}^2/\overline{k}_{r2}\omega$	1.806×10^3
Pe_{r3}	$\rho_{r3}\overline{c}_r\overline{u}^2/\overline{k}_{r3}\omega$	0.748×10^3
Pe_g	$\rho_g\overline{c}_g\overline{u}^2/\overline{k}_g\omega$	1.231×10^3
γ	c_g/c_v	5/3
Subscripts		
b	buffer	
C	cold end	
H	hot end	
g	gas	
r	regenerator	
t	tube	

PREVIOUS PUBLICATIONS IN THIS SERIES:

Number	Author(s)	Title	Month
09-13	J.A.W.M. Groot C.G. Giannopapa R.M.M. Mattheij	Numerical optimisation of blowing glass parison shapes	March '09
09-14	A.S. Tijsseling	Exact computation of the axial vibration of two coupled liquid-filled pipes	May '09
09-15	M. Pisarenco B.J. van der Linden A.S. Tijssseling E. Ory J.A.M. Dam	Friction factor estimation for turbulent flows in corrugated pipes with rough walls	May '09
09-16	B.J. van der Linden E. Ory J.A.M. Dam A.S. Tijsseling M. Pisarenco	Efficient computation of three-dimensional flow in helically corrugated hoses including swirl	May '09
09-17	M.A. Etaati R.M.M. Mattheij A.S. Tijsseling A.T.A.M. de Waele	One-dimensional simulation of a stirling three-stage pulse-tube refrigerator	May '09

Ontwerp: de Tantes,
Tobias Baanders, CWI